



Micro-foaming of plant protein based meat analogues for tailored textural properties

Joël I. Zink^{*}, Liridon Zeneli, Erich J. Windhab

Laboratory of Food Process Engineering, Department of Health Science and Technology, ETH Zurich, Schmelzbergstrasse 9, Zurich, 8092, Switzerland

ARTICLE INFO

Keywords:

meat analogue
High moisture extrusion cooking
Micro-foaming
Plant proteins
Texturization
Tenderness adjustment

ABSTRACT

Meat-like foods based on plant protein sources are supposed to be a solution for a more sustainable sustenance of the world population while also having a great potential to reduce the impact on climate change. However, the transition from animal-based products to more climate-friendly alternatives can only be accomplished when consumers' acceptance of plant-based alternatives is high. This article introduces a novel micro-foaming process for texturized High-Moisture Meat Analogues (HMMA) conferring enhanced structural properties and a new way to tailor the mechanical, appearance and textural characteristics of such products. First, the impact of nitrogen injection and subsequent foaming on processing pressures, temperatures and mechanical energy were assessed using soy protein concentrate and injecting nitrogen fractions in a controlled manner in the range of 0 wt% to 0.3 wt% into the hot protein melt. Direct relationships between related extrusion parameters and properties of extruded HMMA were established. Furthermore, optimized processing parameters for stable manufacturing conditions were identified. Secondly, so produced HMMA foams were systematically analyzed using colourimetry, texture analysis, X-ray micro-tomography (XRT) and by performing water and oil absorption tests. These measurements revealed that perceived lightness, textural hardness, cohesiveness and overrun can be tailored by adapting the injected N₂ concentrations provided that the gas holding capacity of the protein matrix is high enough. Moreover, the liquid absorption properties of the foamed HMMA were greatly optimized. XRT measurements showed that the porosity at the center of the extrudate strands was the highest. The largest porosity of 53% was achieved with 0.2 wt% N₂ injection, whilst 0.3 wt% N₂ lead to destructuration of the HMMA foam structure through limited gas dispersion and wall slip layer formation. The latter can, nonetheless, be improved by adapting the processing parameters. All in all, this novel extrusion microfoaming process opens new possibilities to enhance the structural properties of plant-based HMMA and ultimately, consumers' acceptance.

Credit Author Statement

All authors contributed substantially to this research. Joël Zink (JZ): developed the conceptual framework, developed the scenarios and methodological framework, measured and analyzed the XRT data, interpreted the data, wrote the initial manuscript. Liridon Zeneli (LZ) conducted extrusion experiments and measured and analyzed the textural properties and colour data, edited and commented on the manuscript, supervised the project. Erich Windhab (EW): , interpreted the data, edited and commented on the manuscript, supervised the project.

1. Introduction

The demand for alternative protein sources has soared during the last decade. Indeed, an increasing number of consumers associate their eating habits with climate change, sustainability, animal welfare and personal health.

(Boukid, 2021; Pam Ismail et al., 2020; FAO, 2018; Hagmann et al., 2019; Tukker et al., 2011; Westhoek et al., 2014; Richi et al., 2015; Smetana et al., 2015). Furthermore, new individual economic, social and cultural aspects also affect consumers' decision on purchasing plant-based or other alternative protein sources (Malek et al., 2019; Xazela et al., 2017; Kumar et al., 2017a). This leads to a stream of new meat-like product innovations emerging to satisfy the demand for more

^{*} Corresponding author.

E-mail address: joel.zink@hest.ethz.ch (J.I. Zink).

<https://doi.org/10.1016/j.crf.2023.100580>

Received 6 July 2023; Received in revised form 13 August 2023; Accepted 28 August 2023

Available online 4 September 2023

2665-9271/© 2023 Published by Elsevier B.V. This is an open access article under the CC BY-NC-ND license (<http://creativecommons.org/licenses/by-nc-nd/4.0/>).

environmentally friendly protein-rich foods, but especially also to offer an alternative to animal-based products without compromising consumers' experience. These new meat substitutes aim to mimic the texture, taste, appearance as well as the nutritional values of animal products, which are all crucial factors to persuade consumers to change their eating habits to a more environmentally friendly diet on a daily basis (Weinrich, 2019; Michel et al., 2021; Hoek et al., 2011) and, ultimately, provide a long-term option for a more sustainable sustenance of the growing world population (FAO, 2018; Sabate and Soret, 2014; Norton et al., 2014).

Alternative meat-like protein rich foods, also referred to as Meat Analogues (MA), can be produced from a large variety of different ingredients. For example, meat substitutes from mycoproteins obtained from fungal mass forming proteinaceous fibrous food have already been around since the 80's (Wiebe, 2002). They are generally recognized as a healthy alternative (Denny et al., 2008), but have an environmental impact similar to pork and poultry while also falling into the same price category (Souza Filho et al., 2019; Hashempour-Baltork et al., 2020). Different protein sources that can be textured or incorporated into textured fibrous protein-rich formulations include insects (Smetana et al., 2018), algae (Grahl et al., 2018; Caporgno et al., 2020) and cultured meat (Bhat and Fayaz, 2011; Post, 2012; Bryant, 2020). However, proteins from algal sources have yet to be successfully extracted or processed in a way allowing for optimal product texturization and the reduction or masking off-flavours (Bhuva et al., 2021). Furthermore, insects and cultured meat face low acceptance level issues related to socio-demographic acceptance, food neophobia and food disgust (Onwezen et al., 2019; Dupont and Fiebelkorn, 2020; Iannuzzi et al., 2019; Caparros Megido et al., 2016). Additionally, research is still required to solve technological shortcomings in cell culture production (Chriki and Hocquette, 2020; Choudhury et al., 2020). On the other hand, plant-based HMMAs are the most accepted and sometimes perceived to be more sustainable (Onwezen et al., 2021; Circus and Robison, 2019; De Boer et al., 2013; van der Weele et al., 2019; Estell et al., 2021). Such plant proteins can be sourced from cereals like wheat, pulses such as soy or yellow pea and faba bean, which are legumes (Schreuders et al., 2019; Zhang et al., 2020; Pietrasik et al., 2020; Lam et al., 2016; Du et al., 2018; Cui et al., 2020). Among those, soy concentrates and isolates are the most used due to their favorable gelling properties, availability, price, nutritional quality, consumer perception and functional benefits (Day and Swanson, 2013; Bohrer, 2019; Akdogan, 1999; Kumar et al., 2017b; Hoffman and Falvo, 2004; Onwezen et al., 2021).

Plant protein sources can be structured into fibrous meat-like products using different processes and approaches. Related techniques are manifold and span from 3D printing (Ramachandriah, 2021; Dick et al., 2019) over shear cell technology (Grabowska et al., 2014; Krintiras et al., 2015; Cornet et al., 2021) to electrospinning (Anu Bhushani and Anandharamakrishnan, 2014). An overview over different texturization techniques for HMMAs can be found in recent reviews (Dekkers et al., 2018a; Zhang et al., 2021). On top of all, extrusion is the most used process to produce meat-like products. Especially, high moisture extrusion cooking is widely used due to its cost efficiency, since it applies multiple unit operations at once and, thanks to its high versatility to generate anisotropic fibrous structures. In short, this process, usually operating in a twin-screw configuration, first mixes a protein powder with water and optionally other constituents. In a second step, this mixture is transformed into a liquid protein melt upon heating and intense shearing. Finally, the protein melt is cooled in a cooling die at the end of the extrusion process to harden and synchronously texturize the product by making use of the acting shear and elongation rate acting in the die entrance flow (Harper, 1981; Dekkers et al., 2018a; Banerjee and Bhattacharya, 2012; Akdogan, 1999; Krintiras et al., 2015).

Nonetheless, despite the innovation and research surge to make plant based HMMAs look, taste and as nutritious as their animal models, no product has up to date emerged on the market that fully satisfies all

criteria. This is especially the case regarding product juiciness, crunchiness, textural perception during mastication, handling convenience of the plant-based product and, flavour profile (Osen et al., 2014). The work detailed in the present paper introduces a novel extrusion micro-foaming process that enables the production of meat analogues with tailored structural and textural properties. Indeed, it is well known that while increasing the protein content of foods makes the product more attractive for meat-like extrudates, protein enrichment typically results in harder, chewier and denser textures (Chaiyakul et al., 2009; de Mesa et al., 2009; Kyriakopoulou et al., 2021). This could be counteracted by introducing a finely dispersed gas fraction into the product leading to a tenderization of the extrudate. To our knowledge, this is the first time that nitrogen gas-assisted high moisture extrusion foaming has been used for MAs. Therefore, special attention will be paid to the effect on the gaseous gas injection on processing parameters and its impact on the structural properties of such treated high moisture extruded MAs. The process parameters include the adjustment of pressure and temperature profiles at the extruder endplate as well as along the cooling die and the specific mechanical energy input. Conversely, food foaming by water steam evaporation is a well established method for the production of different extruded products made on maize and wheat dough base (Hayter and Smith, 1988; Samard et al., 2017) as well as for other starch-based extrudates (Khan et al., 2017; Lee et al., 2009). On the other hand, extrusion foaming by gas injection has been extensively researched for polymer applications (Lee et al., 2014; Jin et al., 2019), but the literature is more scarce for food applications, especially regarding injection of gaseous gas into the extruder. Most works focused on the injection of supercritical gases into food melts with subsequently controlled vapor expansion foaming (Cho and Rizvi, 2009; Lee et al., 2009; Chaiyakul et al., 2009). A study closer to this work was performed by Koksel and Masatcioglu (2018), whereby the physical properties of nitrogen assisted extrusion cooking of pea snacks was described. They found a high correlation between extrudate expansion and hardness and, determined that nitrogen gas pressure changed the colour and the degree of expansion of the product. Other works reported entrapped air cavities in unintentionally foamed MAs. Schreuders et al. (2019) measured unintended void fractions of up to 7% in soy based meat-like extrudates while others measured up to 11% (Dekkers et al., 2018b; Jia et al., 2021) in similar high moisture products. Furthermore, a correlation between tensile stress and void fraction was described (Dekkers et al., 2018b). The present paper will in contrast focus on tailored micro-foaming with increased gas fractions and trace micro-bubble foam size distribution and for such, also determine the impact of the void fraction on the mechanical and structural properties of soy-based MAs. Furthermore, the effect of foaming on water and oil absorption is addressed as the flavour as well as the textural properties of HMMAs can be enhanced by post-extrusion marination and soaking of liquid or semi-liquid phases to improve the similarity to animal meat and, ultimately, reach higher consumer acceptance.

2. Material and methods

2.1. Meat analogue extrusion

The foamed and non-foamed high-moisture meat analogue (HMMA) samples were produced using an intermeshing co-rotating twin screw extruder (BCTL D42 32D Polytwin, Bühler AG, CH) with screw diameter D of 42 mm and a extruder length L to screw diameter ratio of $L/D = 32$. Soy protein concentrate powder (SPC) (Alpha-8, Solae LLC, USA) with a protein content of min. 67% and a moisture content of max. 8%, according to the manufacturer, was gravimetrically dosed into the first extruder segment at $L/D = 0$ using a weight-in-loss solid dispenser (K-MLD5-KT35, Coperion K-Tron AG, CH). Canola oil (Florin AG, CH) was injected in the second extruder barrel segment at $L/D = 5.3$ by a progressive cavity pump (Netsch AG, DE) complemented by tap water at room temperature injection at $L/D = 5.7$ involving the use of a

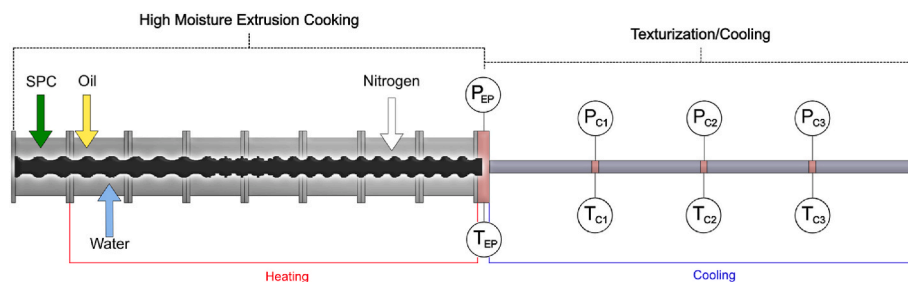


Fig. 1. Schematic representation of a high moisture extrusion cooking (HMEC) process for the production of high-moisture meat analogues depicting the inlets of soy protein concentrate (SPC) powder, oil, water and nitrogen with arrows. The extruder screw, configured with conveying elements, kneading blocks and gear elements for optimal gas dispersion, is shown in black. The three different heating sections of the cooking process are highlighted in red below the extruder. The temperatures of the two texturing zones in the cooling die are shown in blue. Additionally, the position of pressure transducers and temperature sensors are depicted with circles and the letters *P* and *T*, respectively. The subscripts of the sensors give additional information regarding their emplacement, whereby *EP* stands for the extruder endplate and *C1* – *3* for their relative position along the cooling die. (For interpretation of the references to colour in this figure legend, the reader is referred to the Web version of this article.)

peristaltic pump (530 WatsonMarlow Fluid Technology Group, UK). The N_2 gas (Carbagas, CH) inlet was connected to a Coriolis mass flow meter and controller (CORI-FLOW™ M13, Bronkhorst, CH) to ensure a controlled gas feed with a gas injection pressure of 10 barg. The protein melt was heated by pressurized water flowing in the double-jacketed extruder segments up to a temperature of about 140 °C at the extruder end-plate (EP). Finally, the so-produced protein melt was texturized in a cooling die (PolyCool BFTK50, Bühler AG, CH) mounted at the endplate of the extruder. The cooling die with a length of 120 cm was divided into 4 sections, whereby a product temperature sensor and a product pressure transducer were placed between each of the sections to obtain optimal processing information. This extrusion setup is schematically depicted in Fig 1. Moreover, the positions of four temperature sensors and pressure transducers, positioned at the extruder endplate and along the cooling die, used to gain additional information on the cooling domain if the extrusion process are also depicted. Furthermore, the Specific Mechanical

Energy input (SME), denoting the energy require to extrude a unit mass of MA, was recorded for each gas flow rate setting.

All HMMA samples were produced with the same base formulation at a total mass flow rate of 35 $kg\ h^{-1}$ and composed of 38.5 wt% SPC, 57.7 wt% water, and 3.8 wt% oil. To produce non-foamed and foamed samples, gaseous nitrogen fractions of 0 wt%, 0.05 wt%, 0.1 wt% and 0.3 wt% were injected into the protein melt. The screw speed was set to 275 rpm. The so produced samples were sealed inside plastic bags to avoid moisture loss and stored overnight at 4 °C until further analyses. The system parameters, SME, extrudate temperature, and pressures were measured over 10 min once stable processing conditions were reached. The so obtained were arithmetically averaged and the standard deviation calculated values for each injected N_2 gas fraction.

2.2. Soaking with oil and water

To determine the impact of foaming on the water and oil absorption, the HMMA samples were first cut transversally into 20 mm slices. In a second step, the slices were immersed in tap water and canola oil (Florin AG, CH) at room temperature for 5 min prior to sample analysis.

2.3. Sample characterisation

The textural hardness and cohesiveness were assessed using a texture analyzer (TA.XTPlus, Stable Micro Systems, USA) equipped with a cylindrical aluminum probe of 36 mm in diameter. For this, the HMMA extrudates were cut into cylindrical samples with a diameter of 20 mm and a height of 10 mm and compressed twice by 35% of their initial height at a probe speed of 1 $mm\ s^{-1}$ with a time interval of 5 s between the compression cycles. The peak force of the first compression cycle

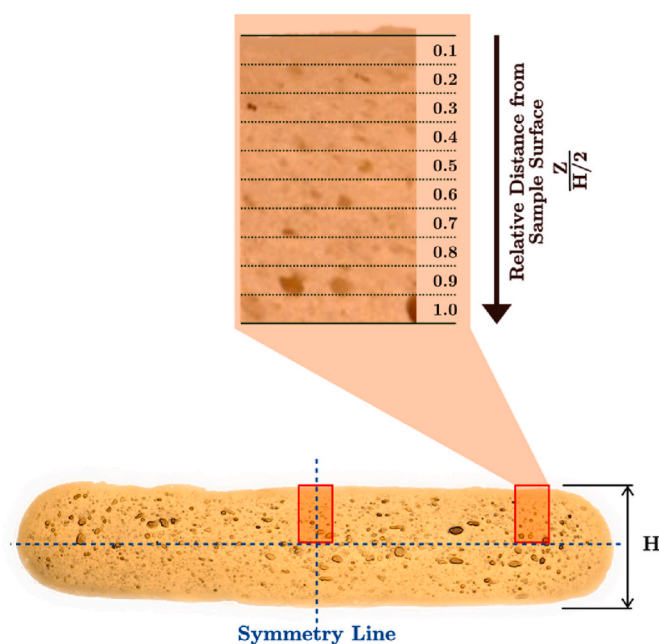


Fig. 2. Bottom: Front view of transversally cut high-moisture meat analogue extrudate schematically depicting the position where cylindrical samples were cut out for μ CT pore size analysis (red rectangles). Vertical and horizontal symmetry lines are shown by blue dashed lines.

Top: Depiction of relative distance from sample surface to the center of the extrudate.

The relative distance is a normalized fraction Z of half of the total sample height H . (For interpretation of the references to colour in this figure legend, the reader is referred to the Web version of this article.)

defined the textural hardness while the cohesiveness was obtained by dividing the area under the second compression peak by the area under the first compression peak.

A chromameter (CR-300, Minolta, JPN) was used to record the change in colour of the HMMA samples upon nitrogen injection and subsequent foaming followed by soaking of oil or water.

The degree of foaming was determined by a custom-made Mohr-Westphal scale constructed out of two main components, namely a wire basket hanging on an electrical scale via a stiff metal rod. With this relatively simple setup, the density of solid samples could be calculated using Archimedes' principle by measuring the weight of the sample in two different fluids with known densities. In this work, the densities of HMMA samples were measured in ambient air and water. For this, the extruded HMMA samples were transversally cut into slices with a

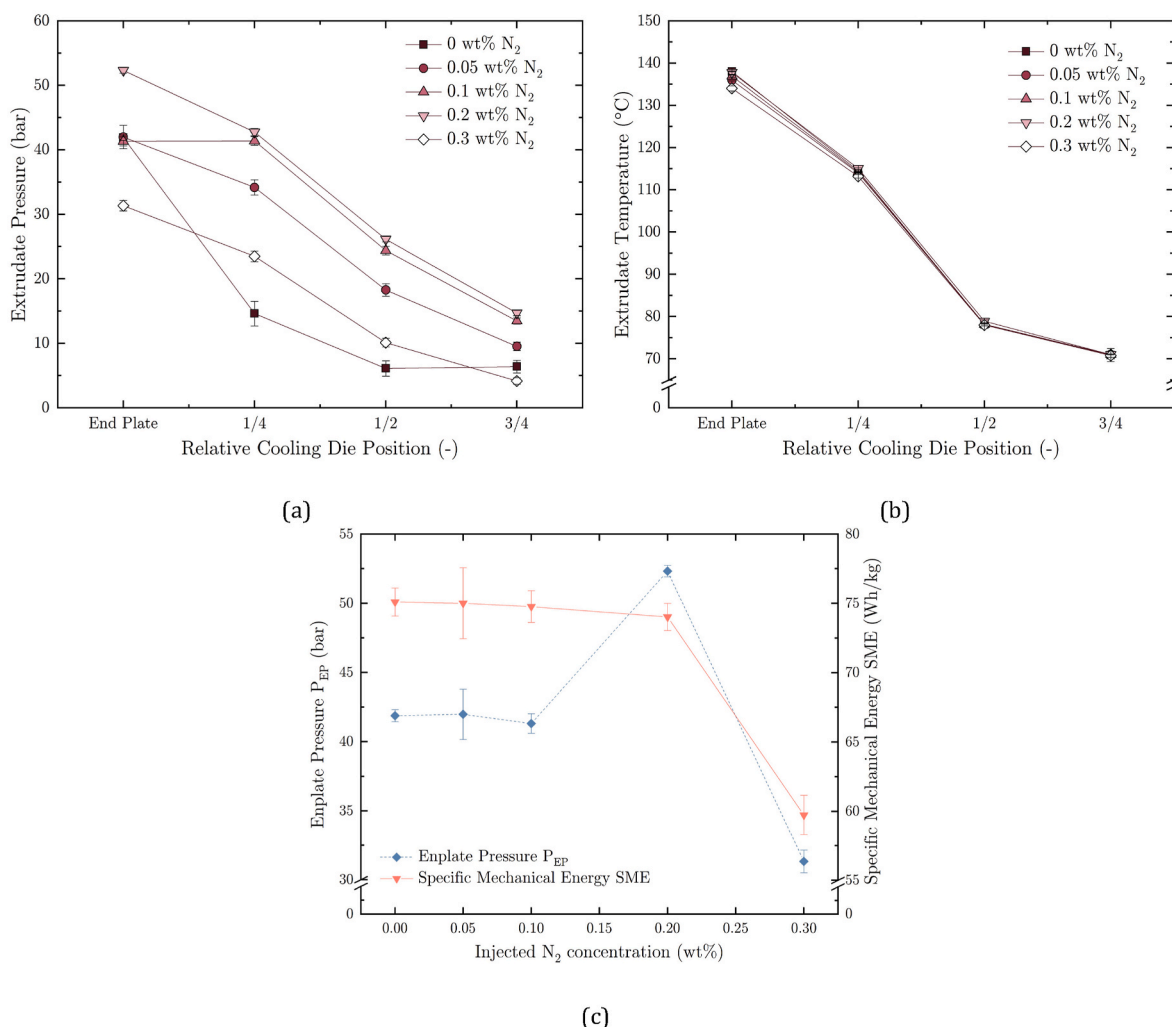


Fig. 3. Evolution of pressure, temperature and specific mechanical energy input for different injected N₂ fractions from 0 wt% to 0.3 wt% at the extruder end-plate as well as along the cooling die as depicted in Fig. 1. Subfigures (a) and (b) show the pressure and the temperatures of the extruded HMMA at the extruder end-plate and in the cooling die. Subfigure (c) depicts the change of the pressure at the end-plate along with the specific mechanical energy input for increasing gas fractions.

thickness of 20 mm and tightly wrapped in cellophane to avoid moisture loss and liquid absorption during the weighing in air and water, respectively. Finally, the overrun (OR) of the foamed HMMA samples was calculated as described by Eq. (1), whereby $\rho_{MA, noa}$ denotes the density of non-aerated samples and $\rho_{MA, aer}$ the density of aerated HMMA extrudates foamed by nitrogen injection as described before.

$$OR = \frac{\rho_{MA, noa} - \rho_{MA, aer}}{\rho_{MA, aer}} * 100 \quad (1)$$

The results of the textural hardness, cohesiveness, colour, and overrun were obtained by measuring five replicates for each injected N₂ gas fraction with and without soaked liquid. The data shown in the result section are the arithmetic means and standard deviations for each parameter set.

Pore size analysis by 3D micro x-ray tomography (XRT) was performed to gain additional insights into the structure of foamed and non-foamed HMMA samples using a cabinet cone-beam (μ CT 100, Scanco Medical AG, CH) set to 90 kV, 88 μ A and 8W and a resolution of 3.3 μ m. For this, two cylindrical cuts with a diameter of 6 mm for each nitrogen injection setting were taken in duplicate at two distinct positions on the extruded product. As depicted in Fig. 2 one sample was cut out at the edge of the HMMA strand and one in the center. The samples taken at the edge were cut out besides the curved part of the strand to produce samples of comparable shape to the ones taken in the center. These

cylindrical samples were then immediately placed into hollow tube sample holders and covered with a paraffin film to minimize moisture loss. As also depicted in Fig. 2, only half of the thickness of the HMMA strand was scanned to shorten scanning time. Hence, a symmetrical flow profile of the protein melt in the cooling die was assumed and visually confirmed for all texturized samples. Furthermore, the results were partitioned into ten slices to identify locally diverging porosities in the foamed HMMA samples. For this, the functionalities of the PoreSpy (Gostick et al., 2019) library were used with python 3.8.

3. Results and discussion

3.1. Impact of N₂ gas injection on system parameters

The impact of gaseous nitrogen injection and the consequential foaming of the plant protein-based High-Moisture Meat Analogue (HMMA) on the extrusion parameters is depicted in Fig. 3. As expected, the injection of nitrogen into the protein melt changed the measured temperature and pressure reading as well as the Specific Mechanical Energy (SME) required to extrude this product. Indeed, while the measured pressures (Fig. 3 (a)) and temperatures (Fig. 3 (b)) of all extruded HMMA formulations showed the typical decreasing trend towards the exit of the cooling die, the pressures were substantially different for different degrees of gas injections. The pressure of the

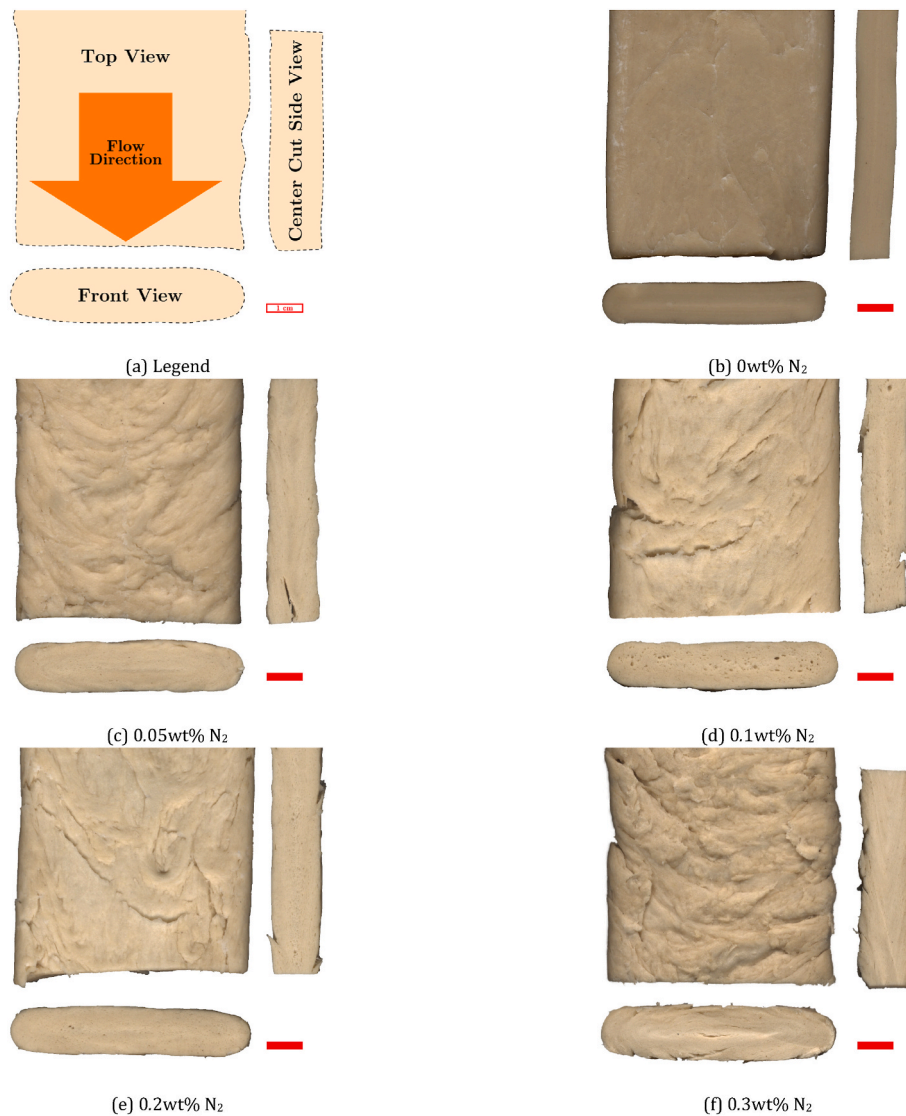


Fig. 4. Captures of produced high-moisture meat analogue samples with different N₂ concentrations ranging from 0 wt% to 0.3 wt% ((b) to (f)). The legend is given by the sub-image (a). Top left: Top view of high-moisture meat analogue as seen when it is exiting the cooling die; Bottom: Front view of transversally cut sample; Right: Side view of sample cut in the extrudate center. Flow direction is from top to bottom. The red bar corresponds to 1 cm. (For interpretation of the references to colour in this figure legend, the reader is referred to the Web version of this article.)

HMMA in the cooling die increased with higher gas fractions up to 0.2 wt%. For the largest injected gas fraction of 0.3 wt% N₂, the recorded pressure was lower at the end-plate as well as at the nearest measuring point to the die outlet. The initial increase in pressure with the gas injection was expected as it is known that foam has typically a higher viscosity than its base liquid and, therefore, a higher resistance to flow is resulting (Hanselmann and Windhab, 1998; Lammers et al., 2017; Zink et al., 2022). Consequently, the pressure of the foamed HMMA increased at the extruder end-plate and in the cooling die. Nonetheless, this is only the case if no slip layer is formed between the foam and the die walls. This was however what partially occurred when 0.3 wt% N₂ were injected, leading to an overall decrease in extrusion pressure. Accordingly, both the pressure at the extruder end-plate and at the nearest measuring point towards the exit of the cooling die were even lower compared to the non-foamed MA. This effect arose through a mixed phenomenon involving (i) a collapse of the HMMA foam through gas bubble coalescence and, (ii) an imperfect gas dispersion leading to the formation of a slip layer by gas-enriched material in the zone of highest acting shear stress at the die wall. Further increasing the gas

fraction lead to a complete destabilization of the extrusion process, as the even lower resistance to flow did no longer generate sufficient back-pressure in the extruder required for appropriate gas dispersion. Conversely, the temperature readings were, apart from some minor differences at the extruder end-plate position, indistinguishable. This is due to the fact that the thermocouples have been placed such that they barely penetrate the extrudate in order to not leave visible traces on the HMMA and minimally disturb the flow profile. The gas-induced extrusion destabilizing effect could also be detected by the SME as depicted along with the extruder endplate pressure in Fig. 3 (c). However, the SME was less affected by the gas content than the pressure when the nitrogen fraction was increased up to 0.2 wt% since it is dominated by high friction forces acting in the extruder feeding and conveying sections where the material has still dry and wet powder flow characteristics. Once 0.3 wt% N₂ were injected, the SME decreased substantially due to incomplete gas dispersion leading to the formation of the gas-enriched pockets and wall slip layer formation. Therefore, it can be concluded that it is sufficient to monitor the SME to determine whether an upper gas injection limit is reached instead of the more costly and time

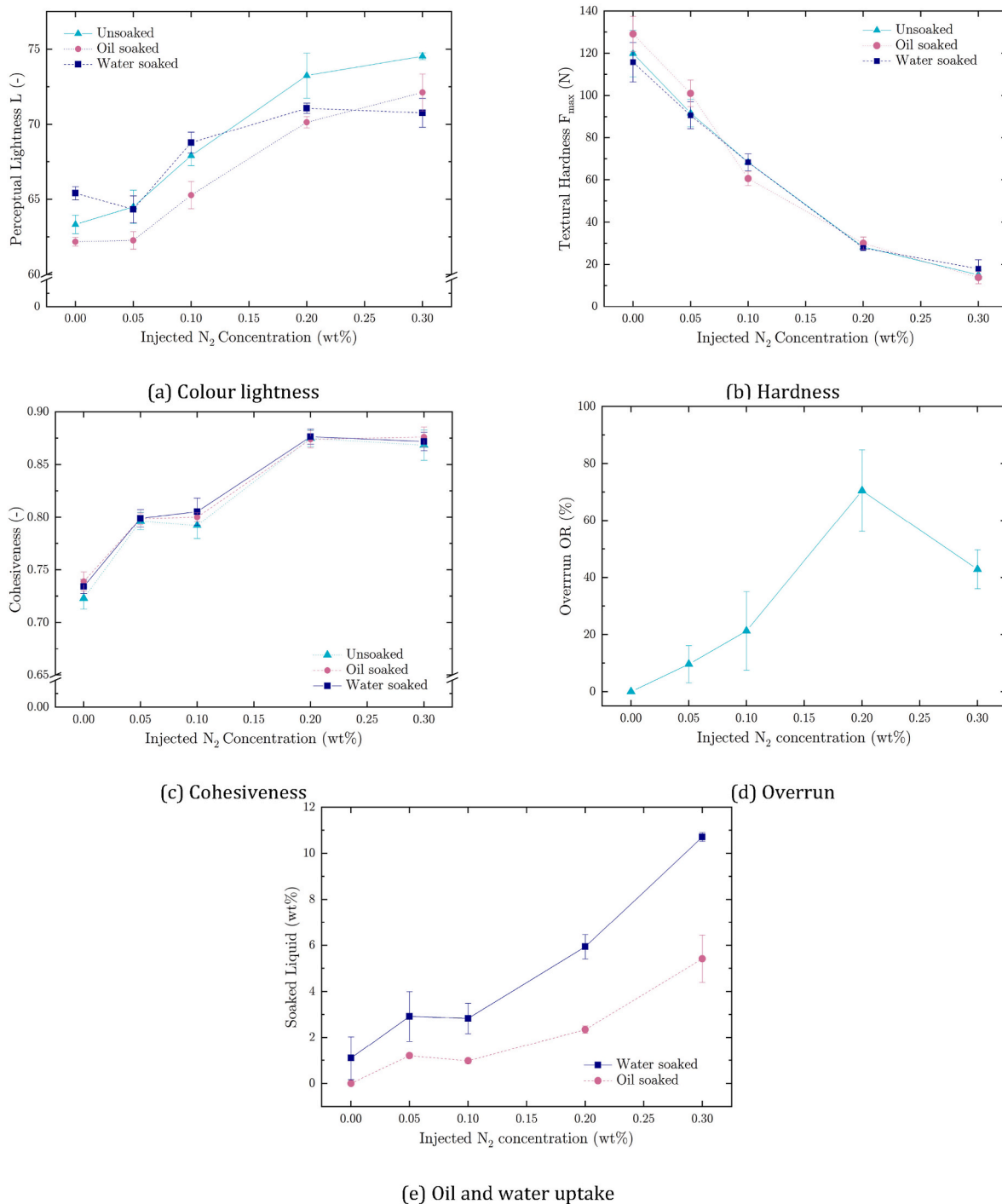


Fig. 5. Perceptual lightness, textural hardness and cohesiveness as well as overrun and liquid absorption characteristics of nitrogen foamed SPC-based high-moisture meat analogues. Extruded samples were soaked in tap water and canola oil prior to texture analysis and colour measurements. (For interpretation of the references to colour in this figure legend, the reader is referred to the Web version of this article.)

intensive recording of the pressure profile along the cooling die. This is of particular interest for an optimal implementation of this new foaming technique into already existing HMMA extrusion processes as the SME or the torque are already being recorded.

3.2. Physical properties of foamed meat analogues

The increase in number of micro bubbles in HMMA samples and the correlating change in protein melt flow can qualitatively be assessed using the naked eye for macro bubbles. As shown in Fig. 4 coloured

HMMA images taken with the same homogeneous light source reveal three visual characteristics that change upon nitrogen injection. Firstly, N₂ injection lead to an overall lightning of the HMMA samples. This effect is due to an enhanced light scattering originating from an increase in surface roughness in the presence of more micro-bubbles and micropores at the surface of the samples. Secondly, the flow disturbances as a result of the increased gas fraction incorporated in the protein matrix lead to a macroscopic coarsening of the surface of the extrudate strands that was more pronounced when the nitrogen injection was increased. Such consequence of the novel foaming process can be used to

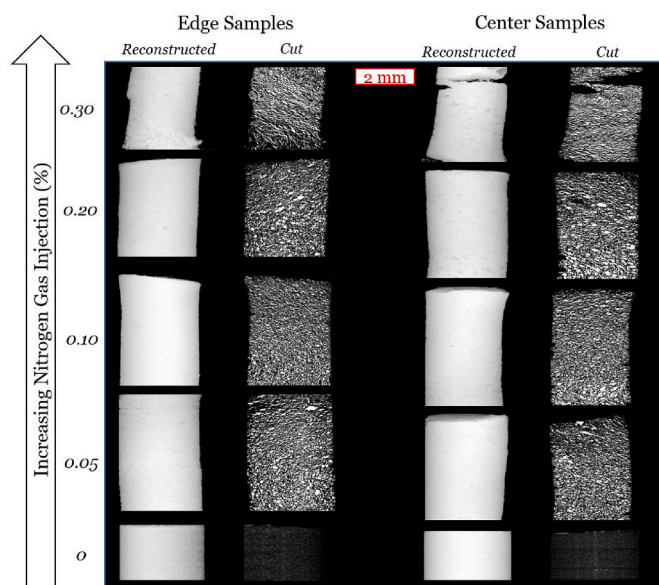


Fig. 6. Images of XRT scanned HMMA samples foamed with 0%–0.3% nitrogen. Cylindrical samples were cut out at the edge of the HMMA strands as well as in the center of the band exiting the cooling die. Reconstructed 3D representations of the scans are next to 2D cuts, whereby the detected pores are shown in white.

accentuate the structural heterogeneity of the product and therefore, widen the palette of meat-like products by introducing new and different textural properties without changing the plant protein-based formulation. The third major visually detectable impact on HMMA arising from nitrogen addition could be observed by cutting the samples transversally and longitudinally to the flow direction of the product exiting the cooling die. As expected, higher injected gas fractions lead to the appearance of more macro bubbles in the HMMA samples. Additionally, the increased number of gas bubbles did not only improve the visibility of the typical parabolic laminar flow profile forming in the cooling die upon solidification of the protein melt but also accentuated a more heterogeneous distribution of gas bubbles throughout the samples.

Indeed, the foamed HMMA samples were lighter in the middle of the extruded strand and darker near the edges hinting at different pore size distributions and depending on sample depth. These differences in bubble sizes could also be the result of more pronounced bubble dispersion closer to the die wall, where higher shear stress is acting proportional to the die width.

The aforementioned change in HMMA sample lightness upon gaseous N_2 injection was also measured using a colourimeter to confirm the qualitative visual assessment with a quantitative method. The results of these measurements are shown in Fig. 5 (a) along with the results for the textural hardness (b) and cohesiveness (c) measurements as well as for the overrun (OR) (d) and for soaked liquid fractions relative to the initial HMMA weight (e). The change in perceptual lightness, described by the L value on the Lab* scale, showed significantly higher values with increasing nitrogen fractions, thus confirming the visual observations. Soaking the HMMA with canola oil darkened the samples at all injected gas fractions, while the water uptake only significantly reduced the lightness of the samples foamed at the two highest nitrogen mass flow rates. Darkening of the HMMAs resulted from the opposite effect that lead to a brightening of the samples previously discussed. Uptaken liquids filled the pores and smoothed the irregularities generated by pores open to the extruded strand surface generated by the foaming process and therefore, lead to reduced light scattering at the surface of the extrudates. The textural hardness as well as cohesiveness were less affected by the soaked oil and water. The textural hardness decreased with increasing N_2 fraction while the cohesiveness increased. This is

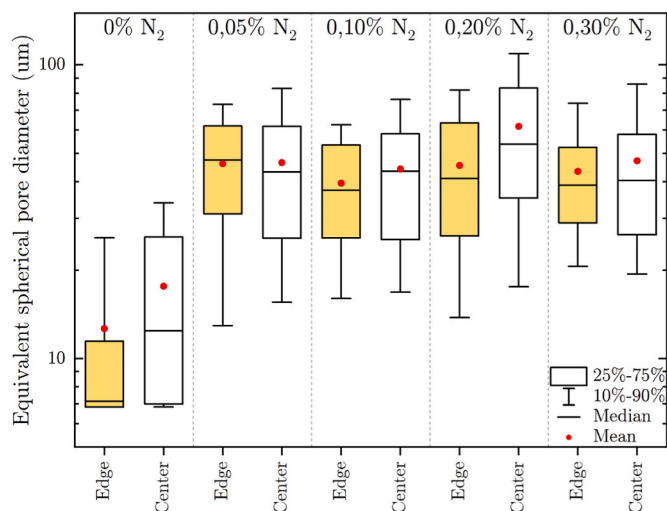


Fig. 7. Equivalent spherical pore diameter of HMMA samples foamed with 0 wt % to 0.3 wt% N_2 during high moisture extrusion. The samples were taken at the edge (yellow box) of the extruded HMMA strand and at the center (empty box) as depicted in Fig. 2 for additional structural information. (For interpretation of the references to colour in this figure legend, the reader is referred to the Web version of this article.)

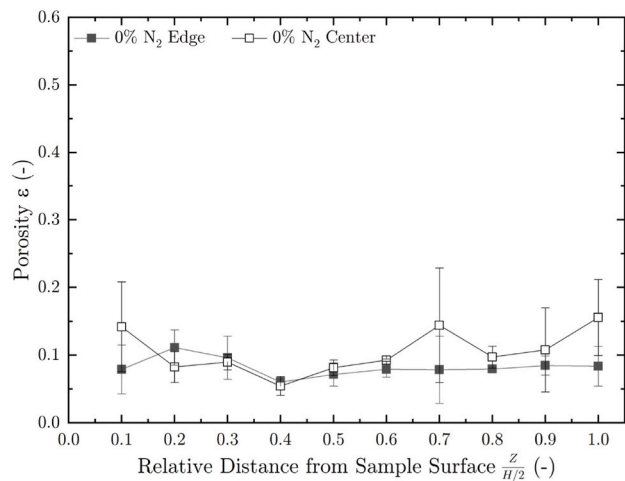
expected to indicate that the foam structure of the HMMAs is of increased compressibility due to the gas bubble inclusions, even though the gas can escape through the fraction of.

open pores upon compression. The soy protein-based network was flexible enough to not break when the uniaxial deformation in that testing device was applied thus, leading to a fast and almost complete recovery of the initially compressed volume at higher gas injections. Conversely, the highest OR of about 70% was reached with 0.2 wt% and not with the maximally tested N_2 content of 0.3 wt%. This supports the conclusions drawn from the readings of the extrusion process parameters discussed in section 3.1. The foam structure collapsed partially when 0.3 wt% N_2 were injected into the HMMA system leading to a drop in extrusion pressure and SME and ultimately, to a lower gas holding capacity probably due to the formation of an increased fraction of open pores. The relative liquid absorption of the foamed HMMA was continuously increasing with the injected N_2 fraction, since open pores support the liquid uptake. Furthermore, the samples were able to absorb both water and oil but with a lesser extend of the latter, indicating that the samples are mostly hydrophilic but are characterized by pores also favoring the uptake of hydrophobic liquids.

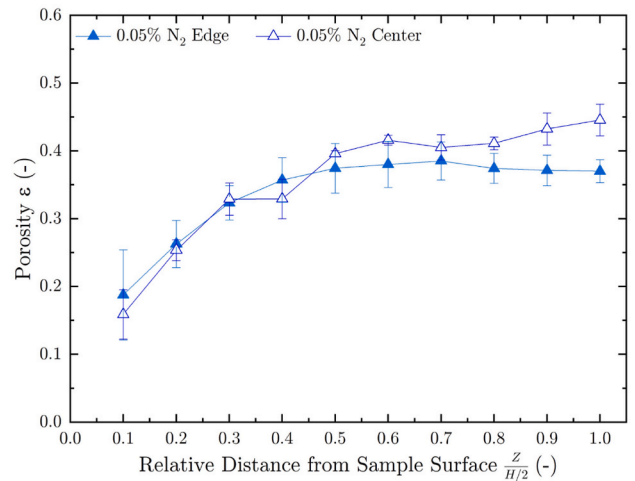
3.3. Porosity and gas bubble distribution of foamed meat analogues

In this section, the results of the pore characterisation of HMMA samples with different foaming degrees measured using high-resolution XRT are shown. The reconstructed 3D representations are depicted along with a 2D cut of the same sample in Fig. 6. This figure shows how sample porosity changes with increasing nitrogen fraction injected during the extrusion process. It is confirmed that the unfoamed samples with no gas injection exhibit very low porosity compared to foamed samples when considering the white surfaces of each cut representing the pores. Moreover, the pores increase in fractions.

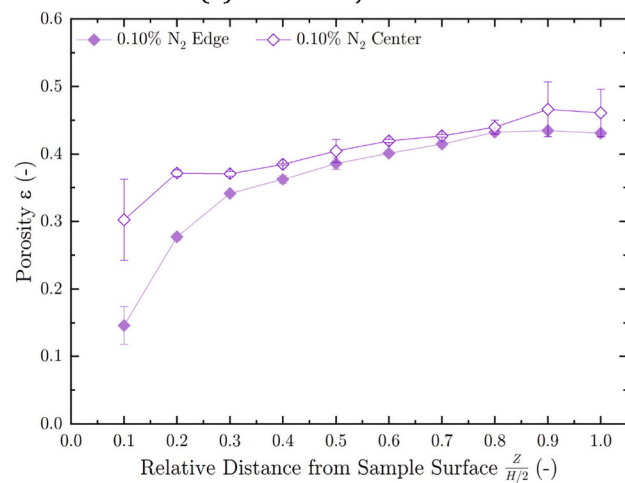
and in size with increasing gas content up to a gas fraction of 0.2%. This is in agreement with the conclusions that more open pores are formed at 0.3% injected gas fraction, thus some overrun getting lost, however liquid uptake being increased. At 0.3% gas dosing one can detect from Fig. 6 more lengthy, stretched pores and lower pore fraction. This is also consistent with the endplate pressure drop observation since material layers next to the cooling die wall with an increased gas fraction from collapsing or opening foam pores support such pressure drop.



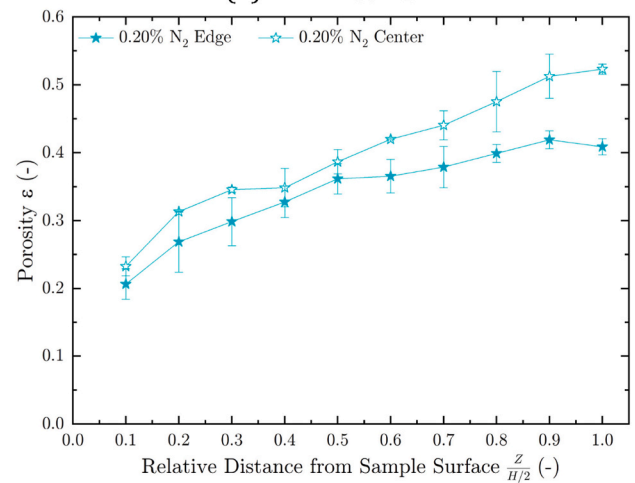
(a) No Gas Injection



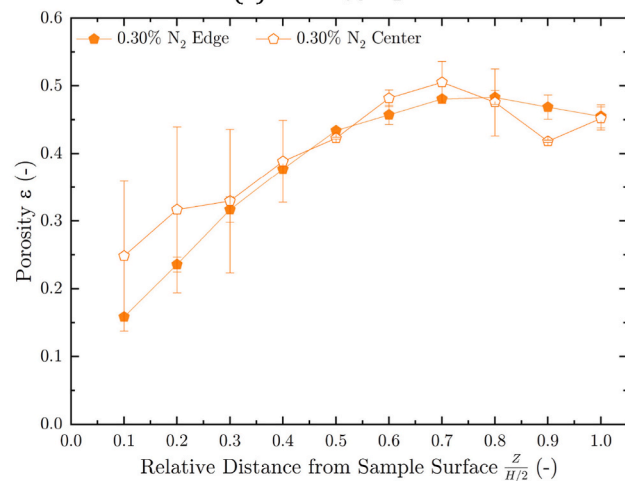
(b) 0.05wt% N₂



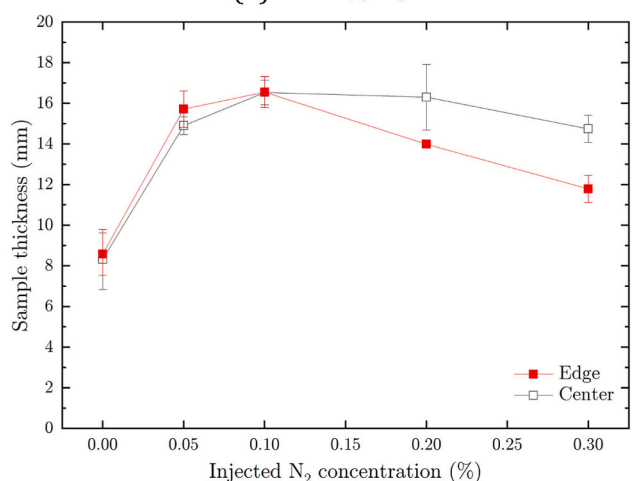
(c) 0.1wt% N₂



(d) 0.2wt% N₂



(e) 0.3wt% N₂



(f) Sample thickness

Fig. 8. Porosity of extrusion foamed HMMA samples with N₂ fractions of 0 wt% to 0.3 wt% in subplots (a)–(e). Filled symbols depict the porosity of samples measured at the edge of the HMMA stands, empty symbols stand for samples measured in the center of the extrudate. The samples were digitally sliced into ten slices representing the relative distance to the surface of the strands. Measured sample thickness values are shown in (f).

The pore size distributions of the HMMA samples foamed using the extrusion aeration process are shown in Fig. 7 and the porosities at relative distance to the sample surface are given in Fig. 8 (a) to (e) along with the sample thickness (f). As described in Fig. 2, the samples were taken from the edge of the HMMA and the center also get information on structural homogeneity within the extrudates. No clear distinctions in pore size distributions could be measured between the foamed samples apart from a slight tendency of increase in the mean value of pore size for the 0.2% gas injection in the sample center. This leads to the assumption that the overall pore size did not substantially increase when more nitrogen was injected, but rather increased the overall number of pores of comparable sizes and thus, also the sample porosity. A related distinction between the samples taken within the same extrudate strand produced with the same parameters could nonetheless be made. In principal, the porosity increased towards the sample center of the HMMA strands compared to the edges. This confirms the findings previously discussed in the scope of this work, whereby the spatial distribution of the acting shear stresses in the cooling die favour the deformation and leakage of foam pores close to the die wall where maximum shear stress is acting. Some related gas fraction loss is indicated by the porosity distribution across the samples as detected. An additional slight tendency of smaller mean bubble diameters in the edge zones of the extruded strands compared to the center zone could be attributed to the increase in the dispersing capability at increased shear stress.

The porosities at different relative sample depths show overall the same tendencies observed for the pore size distributions. The porosity for all foamed HMMA samples increased remarkably with even the lowest injected nitrogen fraction of 0.05 wt% and steadily increased towards the middle of the investigated HMMA strands. Without gas addition, the porosity of the nonfoamed samples were around 10%, which is similar to the findings of (Dekkers et al., 2018b; Jia et al., 2021; Schreuders et al., 2019). In the foamed MA, such low values could only be measured in the parts nearest to the surface of the samples. The highest porosity of 53% was obtained in the center of HMMA samples foamed with a N₂ injection of 0.2 wt%. Again, this correlates with the OR results described previously whereby the highest OR was found for the samples with 0.2 wt%. Furthermore, the sample thickness measurements additionally show that the HMMA stands were the thickest in the middle and thinned towards the curved border. This arises from two main superimposing effects. Firstly, as previously mentioned and discussed, the shear stress near the wall of the cooling die is higher than in the center leading to a decreasing gas bubble dispersion towards the center of the protein melt. Secondly, the melt is cooled from the outside towards the center resulting into a growing foamed solid layer at the wall that is getting thicker along.

the cooling die until, eventually, forming the HMMA strand that exits the die. Hence, gas bubbles in the center of the protein melt have also more time to adapt to the decreasing pressure along the cooling die and thus, expand more compared to the gas bubbles near the wall that have been faster entrapped by the solidifying protein matrix.

4. Conclusion and outlook

In this work, results from detailed structure analyses of High-Moisture Meat Analogues (HMMA) generated in a novel high moisture micro-foaming extrusion cooking process were shown for the first time. The results presented in this paper give indications on the structure tailoring ability of such novel process. Soy protein concentrate based samples have been produced under systematic variation of the parameters with special consideration of the degree of.

N₂-injection based micro-foaming. Resulting samples showed enhanced liquid.

absorption characteristics. More importantly, it was demonstrated that the textural and optical characteristics of meat-like products can be tailored with respect to the instrumentally analyzed structure and

texture parameters, namely porosity, overrun, pore size distribution, liquid soaking ability as well as textural hardness and cohesiveness. The latter two textural characteristics are expected to correlate with the sensory biting and chewing strength perceptions and thus give orientation for future tailoring of HMMA tenderness as one of the main characteristics for the distinction between chicken-to beef-like alternatives. These findings are part of a first development step towards a new generation of texture-tailored meat-like products with higher consumers' acceptance, while also offering improved production versatility and giving more options for future innovations in this food sector.

Declaration of competing interest

We wish to confirm that there are no known conflicts of interest associated with this publication and there has been no significant financial support for this work that could have influenced its outcome.

We confirm that the manuscript has been read and approved by all named authors and that there are no other persons who satisfied the criteria for authorship but are not listed. We further confirm that the order of authors listed in the manuscript has been approved by all of us.

We further confirm that we have given due consideration to the protection of intellectual property associated with this work and that there are no impediments to publication, including the timing of publication, with respect to intellectual property. In so doing we confirm that we have followed the regulations of our institutions concerning intellectual property.

We understand that the Corresponding Author is the sole contact for the Editorial process (including Editorial Manager and direct communications with the office). He is responsible for communicating with the other authors about progress, submissions of revisions and final approval of proofs. We confirm that we have provided a current and correct email address which is accessible by the Corresponding Author.

Data availability

Data will be made available on request.

5. Acknowledgement

This work was financed by the Swiss Commission of Technology and Innovation (CTI). We thank Selina Frei, Valerie Brunner, Christoph Vogel, Christoph Schill and Christoph Naef from Bühler AG for their valuable cooperation in this project. Moreover, we extend our thanks to Lucia Kölle and Elisa Bissaco from the institute for biomechanics of ETH Zurich for the 3D micro x-ray imaging of foamed high-moisture meat analogue samples.

References

- Akdogan, H., 1999. High moisture food extrusion. *Int. J. Food Sci. Technol.* 34, 195–207. <https://doi.org/10.1046/j.1365-2621.1999.00256.x>.
- Anu Bhusani, J., Anandharamakrishnan, C., 2014. Electrospinning and electrospraying techniques: potential food based applications. *Trends Food Sci. Technol.* 38, 21–33. <https://doi.org/10.1016/j.tifs.2014.03.004>.
- Banerjee, S., Bhattacharya, S., 2012. Food gels: gelling process and new applications. *Crit. Rev. Food Sci. Nutr.* 52, 334–346. <https://doi.org/10.1080/10408398.2010.500234>.
- Bhat, Z.F., Fayaz, H., 2011. Prospectus of cultured meat - advancing meat alternatives. *J. Food Sci. Technol.* 48, 125–140. <https://doi.org/10.1007/s13197-010-0198-7>.
- Bhuvra, V., Borah, A., Morya, S., 2021. A review on meat analogue: is this time to see the algal proteins as a sustainable substitute for the meat proteins? *Pharm. Innov.* 10, 1160–1168.
- Bohrer, B.M., 2019. An investigation of the formulation and nutritional composition of modern meat analogue products. *Food Sci. Hum. Wellness* 8, 320–329. <https://doi.org/10.1016/j.fshw.2019.11.006>.
- Boukid, F., 2021. Plant-based meat analogues: from niche to mainstream. *Eur. Food Res. Technol.* 247, 297–308. <https://doi.org/10.1007/s00217-020-03630-9>.
- Bryant, C.J., 2020. Culture, meat, and cultured meat. *J. Anim. Sci.* 98, 1–7. <https://doi.org/10.1093/jas/skaa172>.
- Caparros Megido, R., Gierts, C., Blecker, C., Brostaux, Y., Haubruge, Alabi, T., Francis, F., 2016. Consumer acceptance of insect-based alternative meat products in Western

- countries. *Food Qual. Prefer.* 52, 237–243. <https://doi.org/10.1016/j.foodqual.2016.05.004>.
- Caporgno, M.P., Boöcker, L., Müssner, C., Stirnemann, E., Haberkorn, I., Adelmann, H., Handschin, S., Windhab, E.J., Mathys, A., 2020. Extruded meat analogues based on yellow, heterotrophically cultivated *Auxenochlorella protothecoides* microalgae. *Innovative Food Sci. Emerging Technol.* 59, 102275 <https://doi.org/10.1016/j.ifset.2019.102275>.
- Chaiyakul, S., Jangchud, K., Jangchud, A., Wuttijumngong, P., Winger, R., 2009. Effect of extrusion conditions on physical and chemical properties of high protein glutinous rice-based snack. *LWT - Food Sci. Technol. (Lebensmittel-Wissenschaft -Technol.)* 42, 781–787. <https://doi.org/10.1016/j.lwt.2008.09.011>.
- Cho, K.Y., Rizvi, S.S., 2009. 3D microstructure of supercritical fluid extrudates I: melt rheology and microstructure formation. *Food Res. Int.* 42, 595–602. <https://doi.org/10.1016/j.foodres.2008.12.014>.
- Choudhury, D., Tseng, T.W., Swartz, E., 2020. The business of cultured meat. *Trends Biotechnol.* 38, 573–577. <https://doi.org/10.1016/j.tibtech.2020.02.012>.
- Chriki, S., Hocquette, J.F., 2020. The myth of cultured meat. *Rev.* <https://doi.org/10.3389/fnut.2020.00007>.
- Circus, V.E., Robison, R., 2019. Exploring perceptions of sustainable proteins and meat attachment. *Br. Food J.* 121, 533–545. <https://doi.org/10.1108/BFJ-01-2018-0025>.
- Cornet, S.H.V., Snel, S.J.E., Schreuders, F.K.G., van der Sman, R.G.M., Beyrer, M., van der Goot, A.J., 2021. Thermo-mechanical processing of plant proteins using shear cell and high-moisture extrusion cooking. *Crit. Rev. Food Sci. Nutr.* 1–18. <https://doi.org/10.1080/10408398.2020.1864618>.
- Cui, L., Bandillo, N., Wang, Y., Ohm, J.B., Chen, B., Rao, J., 2020. Functionality and structure of yellow pea protein isolate as affected by cultivars and extraction pH. *Food Hydrocolloids* 108, 106008. <https://doi.org/10.1016/j.foodhyd.2020.106008>.
- Day, L., Swanson, B.G., 2013. Functionality of protein-fortified extrudates. *Compr. Rev. Food Sci. Food Saf.* 12, 546–564. <https://doi.org/10.1111/1541-4337.12023>.
- De Boer, J., Schöler, H., Boersema, J.J., 2013. Motivational differences in food orientation and the choice of snacks made from lentils, locusts, seaweed or “hybrid” meat. *Food Qual. Prefer.* 28, 32–35. <https://doi.org/10.1016/J.FOODQUAL.2012.07.008>.
- de Mesa, N.J.E., Alavi, S., Singh, N., Shi, Y.C., Dogan, H., Sang, Y., 2009. Soy protein-fortified expanded extrudates: baseline study using normal corn starch. *J. Food Eng.* 90, 262–270. <https://doi.org/10.1016/j.jfoodeng.2008.06.032>.
- Dekkers, B.L., Boom, R.M., van der Goot, A.J., 2018a. Structuring processes for meat analogues. *Trends Food Sci. Technol.* 81, 25–36. <https://doi.org/10.1016/j.tifs.2018.08.011>.
- Dekkers, B.L., Hamoen, R., Boom, R.M., van der Goot, A.J., 2018b. Understanding fiber formation in a concentrated soy protein isolate - pectin blend. *J. Food Eng.* 222, 84–92. <https://doi.org/10.1016/j.jfoodeng.2017.11.014>.
- Denny, A., Aisbitt, B., Lunn, J., 2008. Mycoprotein and health. *Nutr. Bull.* 33, 298–310. <https://doi.org/10.1111/j.1467-3010.2008.00730.x>.
- Dick, A., Bhandari, B., Prakash, S., 2019. 3D printing of meat. *Meat Sci.* 153, 35–44. <https://doi.org/10.1016/j.meatsci.2019.03.005>.
- Du, M., Xie, J., Gong, B., Xu, X., Tang, W., Li, X., Li, C., Xie, M., 2018. Extraction, physicochemical characteristics and functional properties of Mung bean protein. *Food Hydrocolloids* 76, 131–140. <https://doi.org/10.1016/j.foodhyd.2017.01.003>.
- Dupont, J., Fiebelkorn, F., 2020. Attitudes and acceptance of young people toward the consumption of insects and cultured meat in Germany. *Food Qual. Prefer.* 85 <https://doi.org/10.1016/J.FOODQUAL.2020.103983>.
- Estell, M., Hughes, J., Grafenauer, S., 2021. Plant protein and plant-based meat alternatives: consumer and nutrition professional attitudes and perceptions. *Sustainability* 13, 1–18. <https://doi.org/10.3390/su13031478>.
- FAO, 2018. World Livestock: Transforming the Livestock Sector through the Sustainable Development Goals. <https://doi.org/10.4060/ca1201en>.
- Gostick, J., Khan, Z., Tranter, T., Kok, M., Agnaou, M., Sadeghi, M., Jervis, R., 2019. PoreSpy: a Python toolkit for quantitative analysis of porous media images. *J. Open Source Softw.* 4, 1296. <https://doi.org/10.21105/joss.01296>.
- Grabowska, K.J., Tekidou, S., Boom, R.M., van der Goot, A.J., 2014. Shear structuring as a new method to make anisotropic structures from soy–gluten blends. *Food Res. Int.* 64, 743–751. <https://doi.org/10.1016/J.FOODRES.2014.08.010>.
- Grahl, S., Palanisamy, M., Strack, M., Meier-Dinkel, L., Toepfl, S., Mörlein, D., 2018. Towards more sustainable meat alternatives: how technical parameters affect the sensory properties of extrusion products derived from soy and algae. *J. Clean. Prod.* 198, 962–971. <https://doi.org/10.1016/j.jclepro.2018.07.041>.
- Hagmann, D., Siegrist, M., Hartmann, C., 2019. Meat avoidance: motives, alternative proteins and diet quality in a sample of Swiss consumers. *Publ. Health Nutr.* 22, 2448–2459. <https://doi.org/10.1017/S1368980019001277>.
- Hanselmann, W., Windhab, E., 1998. Flow characteristics and modelling of foam generation in a continuous rotor/stator mixer. *J. Food Eng.* 38, 393–405. [https://doi.org/10.1016/S0260-8774\(98\)00129-0](https://doi.org/10.1016/S0260-8774(98)00129-0).
- Harper, J.M., 1981. *Extrusion of Foods*. CRC PRESS.
- Hashempour-Baltork, F., Khosravi-Darani, K., Hosseini, H., Farshi, P., Reihani, S.F.S., 2020. Mycoproteins as safe meat substitutes. *J. Clean. Prod.* 253 <https://doi.org/10.1016/J.JCLEPRO.2020.119958>.
- Hayter, A.L., Smith, A.C., 1988. The mechanical properties of extruded food foams. *J. Mater. Sci.* 23, 736–743. <https://doi.org/10.1007/BF01174714>.
- Hoek, A.C., van Boekel, M.A., Voordouw, J., Luning, P.A., 2011. Identification of new food alternatives: how do consumers categorize meat and meat substitutes? *Food Qual. Prefer.* 22, 371–383. <https://doi.org/10.1016/J.FOODQUAL.2011.01.008>.
- Hoffman, J.R., Falvo, M.J., 2004. Protein - which is best? *J. Sports Sci. Med.* 3, 118–130.
- Iannuzzi, E., Sisto, R., Nigro, C., 2019. The willingness to consume insect-based food: an empirical research on Italian consumers. *Agric. Econ.* 65, 454–462. <https://doi.org/10.17221/87/2019AGRIC ECON>.
- Jia, W., Curubeto, N., Rodríguez-Alonso, E., Keppler, J.K., van der Goot, A.J., 2021. Rapeseed protein concentrate as a potential ingredient for meat analogues. *Innovative Food Sci. Emerging Technol.* 72, 1466–8564. <https://doi.org/10.1016/j.ifset.2021.102758>.
- Jin, F.L., Zhao, M., Park, M., Park, S.J., 2019. Recent trends of foaming in polymer processing: a review. *Polymers* 11. <https://doi.org/10.3390/polym11060953>.
- Khan, B., Bilal Khan Niazi, M., Samin, G., Jahan, Z., 2017. Thermoplastic Starch: A Possible Biodegradable Food Packaging Material—A Review. <https://doi.org/10.1111/jfpe.12447>.
- Koksel, F., Masatcioglu, M.T., 2018. Physical properties of puffed yellow pea snacks produced by nitrogen gas assisted extrusion cooking. *Lebensm. Wiss. Technol.* 93, 592–598. <https://doi.org/10.1016/j.lwt.2018.04.011>.
- Krintiras, G.A., Göbel, J., Van Der Goot, A.J., Stefanidis, G.D., 2015. Production of structured soy-based meat analogues using simple shear and heat in a Couette Cell. *J. Food Eng.* 160, 34–41. <https://doi.org/10.1016/J.JFOODENG.2015.02.015>.
- Kumar, P., Chatli, M.K., Mehta, N., Singh, P., Malav, O.P., Verma, A.K., 2017a. Meat analogues: health promising sustainable meat substitutes. *Crit. Rev. Food Sci. Nutr.* 57, 923–932. <https://doi.org/10.1080/10408398.2014.939739>.
- Kumar, P., Chatli, M.K., Mehta, N., Singh, P., Malav, O.P., Verma, A.K., 2017b. Meat analogues: health promising sustainable meat substitutes. *Crit. Rev. Food Sci. Nutr.* 57, 923–932. <https://doi.org/10.1080/10408398.2014.939739>.
- Kyriakopoulou, K., Keppler, J.K., van der Goot, A.J., 2021. Functionality of Ingredients and Additives in Plant-Based Meat Analogues. <https://doi.org/10.3390/foods10030600>.
- Lam, A.C., Can Karaca, A., Tyler, R.T., Nickerson, M.T., 2016. Pea Protein Isolates: Structure, Extraction, and Functionality. *vol. 34*, pp. 126–147. <https://doi.org/10.1080/87559129.2016.1242135>.
- Lammers, V.R.G., Morant, A., Wemmer, J., Windhab, E.J., 2017. High pressure foaming properties of carbon dioxide-saturated emulsions. *Rheol. Acta* 56, 841–850. <https://doi.org/10.1007/s00397-017-1035-y>.
- Lee, S.Y., Eskridge, K.M., Koh, W.Y., Hanna, M.A., 2009. Evaluation of ingredient effects on extruded starch-based foams using a supersaturated split-plot design. *Ind. Crop. Prod.* 29, 427–436. <https://doi.org/10.1016/j.indcrop.2008.08.003>.
- Lee, S.T., Park, C.B., Park, S.T.L., C, B., 2014. *Foam Extrusion Principles and Practice*, second ed. CRC Press, Boca Raton.
- Malek, L., Umberger, W.J., Goddard, E., 2019. Committed vs. uncommitted meat eaters: understanding willingness to change protein consumption. *Appetite* 138, 115–126. <https://doi.org/10.1016/J.APPET.2019.03.024>.
- Michel, F., Hartmann, C., Siegrist, M., 2021. Consumers' associations, perceptions and acceptance of meat and plant-based meat alternatives. *Food Qual. Prefer.* 87, 104063 <https://doi.org/10.1016/J.FOODQUAL.2020.104063>.
- Norton, J.E., Wallis, G.A., Spyropoulos, F., Lillford, P.J., Norton, I.T., 2014. Plant-based proteins: the good, bad, and ugly. *Annu. Rev. Food Sci. Technol.* 5, 177–195. <https://doi.org/10.1146/annurev-food-092221>.
- Onwezen, M.C., van den Puttelaar, J., Verain, M.C., Veldkamp, T., 2019. Consumer acceptance of insects as food and feed: the relevance of affective factors. *Food Qual. Prefer.* 77, 51–63. <https://doi.org/10.1016/j.foodqual.2019.04.011>.
- Onwezen, M.C., Bouwman, E.P., Reinders, M.J., Dagevos, H., 2021. A systematic review on consumer acceptance of alternative proteins: pulses, algae, insects, plant-based meat alternatives, and cultured meat. *Appetite* 159, 105058. <https://doi.org/10.1016/j.appet.2020.105058>.
- Osen, R., Toelstede, S., Wild, F., Eisner, P., Schweiggert-Weisz, U., 2014. High moisture extrusion cooking of pea protein isolates: raw material characteristics, extruder responses, and texture properties. *J. Food Eng.* 127, 67–74. <https://doi.org/10.1016/j.jfoodeng.2013.11.023>.
- Pam Ismail, B., Senaratne-Lenagala, L., Stube, A., Brackenridge, A., 2020. Protein demand: review of plant and animal proteins used in alternative protein product development and production. *Animal Frontiers* 10, 53–63. <https://doi.org/10.1093/af/vfaa040>.
- Pietrasik, Z., Sigvaldson, M., Soladoye, O.P., Gaudette, N.J., 2020. Utilization of pea starch and fibre fractions for replacement of wheat crumb in beef burgers. *Meat Sci.* 161, 107974 <https://doi.org/10.1016/j.meatsci.2019.107974>.
- Post, M.J., 2012. Cultured meat from stem cells: challenges and prospects. *Meat Sci.* 92, 297–301. <https://doi.org/10.1016/j.meatsci.2012.04.008>.
- Ramachandriah, K., 2021. Potential development of sustainable 3D-printed meat analogues: a review. *Sustainability* 13, 938. <https://doi.org/10.3390/su13020938>.
- Richi, E.B., Baumer, B., Conrad, B., Darioli, R., Schmid, A., Keller, U., 2015. Health risks associated with meat consumption: a review of epidemiological studies. *Int. J. Vitam. Nutr. Res.* 85, 70–78. <https://doi.org/10.1024/0300-9831/a000224>.
- Sabate, J., Soret, S., 2014. Sustainability of plant-based diets: back to the future. *Am. J. Clin. Nutr.* 100, 476S–482S. <https://doi.org/10.3945/ajcn.113.071522>.
- Samard, S., Singkhornart, S., Ryu, G.H., 2017. Effects of extrusion with CO₂ injection on physical and antioxidant properties of cornmeal-based extrudates with carrot powder. *Food Sci. Biotechnol.* 26, 1301–1311. <https://doi.org/10.1007/s10068-017-0184-1>.
- Schreuders, F.K., Dekkers, B.L., Bodnár, I., Erni, P., Boom, R.M., van der Goot, A.J., 2019. Comparing structuring potential of pea and soy protein with gluten for meat analogue preparation. *J. Food Eng.* 261, 32–39. <https://doi.org/10.1016/j.jfoodeng.2019.04.022>.
- Smetana, S., Mathys, A., Knoch, A., Heinz, V., 2015. Meat alternatives: life cycle assessment of most known meat substitutes. *Int. J. Life Cycle Assess.* 20, 1254–1267. <https://doi.org/10.1007/s11367-015-0931-6>.
- Smetana, S., Ashtari Larki, N., Pernutz, C., Franke, K., Bindrich, U., Toepfl, S., Heinz, V., 2018. Structure design of insect-based meat analogs with high-moisture extrusion. *J. Food Eng.* 229, 83–85. <https://doi.org/10.1016/j.jfoodeng.2017.06.035>.

- Souza Filho, P.F., Andersson, D., Ferreira, J.A., Taherzadeh, M.J., 2019. Mycoprotein: environmental impact and health aspects. *World J. Microbiol. Biotechnol.* 35, 147. <https://doi.org/10.1007/s11274-019-2723-9>.
- Tukker, A., Goldbohm, R.A., De Koning, A., Verheijden, M., Kleijn, R., Wolf, O., Pérez-Domínguez, I., Rueda-Cantucho, J.M., 2011. Environmental impacts of changes to healthier diets in Europe. *Ecol. Econ.* 70, 1776–1788. <https://doi.org/10.1016/j.ecolecon.2011.05.001>.
- van der Weele, C., Feindt, P., Jan van der Goot, A., van Mierlo, B., van Boekel, M., 2019. Meat alternatives: an integrative comparison. *Trends Food Sci. Technol.* 88, 505–512. <https://doi.org/10.1016/j.tifs.2019.04.018>.
- Weinrich, R., 2019. Opportunities for the adoption of health-based sustainable dietary patterns: a review on consumer research of meat substitutes. *Sustainability* 11, 4028. <https://doi.org/10.3390/su11154028>.
- Westhoek, H., Lesschen, J.P., Rood, T., Wagner, S., De Marco, A., Murphy- Bokern, D., Leip, A., van Grinsven, H., Sutton, M.A., Oenema, O., 2014. Food choices, health and environment: effects of cutting Europe's meat and dairy intake. *Global Environ. Change* 26, 196–205. <https://doi.org/10.1016/j.gloenvcha.2014.02.004>.
- Wiebe, M., 2002. Myco-protein from fusarium venenatum: a well-established product for human consumption. *Appl. Microbiol. Biotechnol.* 58, 421–427. <https://doi.org/10.1007/s00253-002-0931-x>.
- Xazela, N.M., Hugo, A., Marume, U., Muchenje, V., 2017. Perceptions of rural consumers on the aspects of meat quality and health implications associated with meat consumption. *Sustainability* 9 (830 9), 830. <https://doi.org/10.3390/SU9050830>, 2017.
- Zhang, J., Liu, L., Jiang, Y., Shah, F., Xu, Y., Wang, Q., 2020. High-moisture extrusion of peanut protein-/carrageenan/sodium alginate/wheat starch mixtures: effect of different exogenous polysaccharides on the process forming a fibrous structure. *Food Hydrocolloids* 99. <https://doi.org/10.1016/j.foodhyd.2019.105311>.
- Zhang, T., Dou, W., Zhang, X., Zhao, Y., Zhang, Y., Jiang, L., Sui, X., 2021. The Development History and Recent Updates on Soy Protein-Based Meat Alternatives. <https://doi.org/10.1016/j.tifs.2021.01.060>.
- Zink, J., Roth, A., Junker, N., Windhab, E., 2022. Native corn and potato starch as CO₂ gas bubble nucleation agent for low-temperature high pressure foaming applications. *Chemical Engineering Journal Advances* 9, 100211. <https://doi.org/10.1016/j.cej.2021.100211>.